



# Raman spectroscopy of carbon doped MgB<sub>2</sub> prepared using carbon encapsulated boron as precursor



Dinesh Kumar<sup>a</sup>, M. Muralidhar<sup>b</sup>, Masaki Higuchi<sup>b</sup>, M.S. Ramachandra Rao<sup>a,\*</sup>,  
Masato Murakami<sup>b</sup>

<sup>a</sup> Department of Physics, Nano Functional Materials Technology Centre (NFMTC), Materials Science Research Centre (MSRC), Indian Institute of Technology Madras (IITM), Chennai 600036, India

<sup>b</sup> Superconducting Materials Laboratory, Graduate School of Science and Engineering, Shibaura Institute of Technology, 3-7-5 Toyosu, Koto-ku, Tokyo 135-8548, Japan

## ARTICLE INFO

### Article history:

Received 8 March 2017

Received in revised form

3 June 2017

Accepted 5 June 2017

Available online 8 June 2017

### Keywords:

Carbon encapsulated boron

Raman spectroscopy

Critical current density

## ABSTRACT

We have studied the surface topographical changes and the Raman spectroscopic modifications for carbon-doped MgB<sub>2</sub> that was fabricated with carbon-encapsulated boron as precursor. Bulk MgB<sub>2</sub> samples of 20 mm diameter and 7 mm thickness were prepared by an in-situ one-step solid state sintering technique. It was found that optimum doping led to the reduction of the average grain size, which was then effective in enhancing flux pinning in MgB<sub>2</sub>. For the optimum doped sample, the self-field critical current density  $J_c$  at 20 K reached 375 kA/cm<sup>2</sup>. However,  $T_c$  values were suppressed with further carbon doping, presumably due to an increase in the disorder in the system, which was demonstrated by a decrease in full width and half maxima of the  $E_{2g}$  mode in the Raman spectra.

© 2017 Elsevier B.V. All rights reserved.

## 1. Introduction

MgB<sub>2</sub> has the highest  $T_c$  of 39 K among the known metallic superconductors and its discovery [1] has allowed this material to emerge as a promising candidate for various superconducting applications [2,3]. One such attractive application is bulk superconducting magnet, which requires mass production for the commercialization and industrial use. With an added advantage of the low fabrication cost, MgB<sub>2</sub> presents itself as a suitable candidate for many superconducting applications [2,4]. MgB<sub>2</sub> possesses AlB<sub>2</sub> structure where the hexagonally arranged planar boron atoms are connected by the strong intralayer  $\sigma$  bonds [5]. It is widely believed that the coupling of the  $\sigma$  bond vibrations with holes is responsible for superconductivity in MgB<sub>2</sub>. Basically, superconductivity in this system is of a BCS-type and the formation of Cooper pairs is via phonon exchange [6,7]. A multi-gap nature of MgB<sub>2</sub> has been proposed and this has been supplemented by various experimental observations [8,9].

Vibrational dynamics of boron atoms can well be analyzed by Raman spectroscopy [10,11]. Group theory predicts the presence of

four vibrational modes in MgB<sub>2</sub> at the zone centre: asymmetric vibration of the B atoms along the c-axis in the opposite direction,  $B_{1g}$ , a silent mode; asymmetric vibration of the B atoms in the ab-plane,  $E_{2g}$ , a Raman active mode; symmetric vibration of the B atoms and Mg atoms sliding against each other,  $A_{2u}$ , an IR active mode and a symmetric vibration of the B and Mg atoms sliding against each other in the ab-plane,  $E_{1u}$ , an IR active mode. The  $E_{2g}$  mode in MgB<sub>2</sub> couples with the holes in the  $\sigma$  band for the formation of Cooper pairs [9,11–14]. This has been confirmed by various *ab-initio* calculations where the Eliashberg function is found to be maximum at 520–630 cm<sup>-1</sup> [6,15,16] which is indeed close to the vibrational frequencies of the in-plane B vibrations (~600 cm<sup>-1</sup>). Furthermore, Raman spectroscopy can provide important information on disorder and phase segregation in a system [17,18]. Although attempts to improve the  $T_c$  in MgB<sub>2</sub> has not been successful,  $J_c$  can be improved significantly by a proper choice of dopant species, doping concentrations or the growth conditions [19–23]. To improve  $J_c$ , carbon doping is widely used with graphene [24], SiC [25] or carbohydrates [20] as the carbon source which has, up to a certain extent, helped realize higher  $J_c$ . However, to achieve the true potential of MgB<sub>2</sub> in terms of its current carrying capacity and its mechanical strength, further doping efficiency and dopant homogeneity need to be achieved.

A significant progress has been made during the recent years in

\* Corresponding author.

E-mail address: [msrrao@iitm.ac.in](mailto:msrrao@iitm.ac.in) (M.S. Ramachandra Rao).

terms of the processing techniques [2,21–23,26] and doping efficiency [20,27–29] so as to improve  $J_c$ , an important parameter that measures the current that a superconductor can hold in the presence of an applied magnetic field. For the doped  $\text{MgB}_2$ , it is suggested that the defects formed in  $\text{MgB}_2$  act as the effective pinning centres for the magnetic flux lines and thus flux flow can be arrested. Recently, the focus has been on achieving uniform doping of carbon by using carbon encapsulated boron (CEB) as a boron precursor [27]. It was found that  $J_c$  improves by introduction of CEB as a dopant in  $\text{MgB}_2$  [30,31,34]. Therefore, systematic topographical and Raman spectroscopy investigations on a wide range of systematically CEB doped  $\text{MgB}_2$  is necessary.

In the present work, we show the effects of homogeneous carbon doping on the superconducting properties of  $\text{MgB}_2$ . Homogeneous carbon doping was achieved by using CEB with various C content as the precursor. A set of systematically doped samples are subjected to surface topographical and Raman spectroscopy studies. The change in  $J_c$  and  $T_c$  as a function of doping concentration are correlated with the variation in the grain size and the change in the Raman signals.

## 2. Experimental details

Polycrystalline  $\text{MgB}_2$  samples, 20 mm in diameter and 7 mm in thickness, were synthesised using a single-step solid state reaction process. For the undoped  $\text{MgB}_2$  sample, high purity commercial Mg powders and amorphous boron powders (Furuuchi Chemical Corporation, Japan) were ground in the ratio of Mg:B = 1:2. Whereas for the doped samples we used commercial CEB powders with various carbon contents viz. 2.8, 4.5, 7.3, 12.0, and 16.5 wt% (Pavezyum Advance Chemicals, Turkey) and these powders along with the Mg powders were thoroughly ground in a glovebox under  $\text{N}_2$  atmosphere and pressed into pellets using an isostatic pressing machine. The resulting pellets were then wrapped using Ta sheets and subjected to a sintering process at 805 °C for 3 h in flowing Argon gas and finally cooled at a rate of 100 °C/h. Further details on the sample preparation processes can be found elsewhere [34].

Phase purity and the lattice parameters of the fabricated  $\text{MgB}_2$  samples were characterized with a high resolution X-ray diffractometer (Rigaku) using Cu K $\alpha$  radiation in a wavelength of 1.5418 Å. Microstructures of the samples were probed using an atomic force microscope (Hitachi Model AFM5100N) in the contact mode. Raman spectroscopic measurements were performed using a Raman spectrometer (Jobin-Yvon, Horiba Labram) equipped with 532 nm laser and with 1800 gr/mm grating. Magnetic measurements for the determination of  $T_c$  and  $J_c$  were carried out using a SQUID magnetometer (Quantum Design), for which the samples with dimensions of  $1.5 \times 1.5 \times 0.5 \text{ cm}^3$  were cut from the pellet for the measurements.

## 3. Results and discussion

### 3.1. Superconducting properties

Fig. 1 shows plots of  $a$ -axis lattice parameters against the carbon content in CEB precursor. One can see a systematic decrease in the lattice parameter with increasing carbon content, which is due to carbon substitution on the boron site. A smaller atomic radius of carbon (0.77 pm) as compared to that of boron (0.88 pm) results in the  $a$ -axis lattice contraction when boron atoms are replaced by the carbon atoms [32,33]. We did not see such contractions in the  $c$ -lattice parameter, suggesting that the Mg atoms remain relatively unaffected, further details on this can be found elsewhere [34]. This is consistent with the results from the earlier work in carbon-doped  $\text{MgB}_2$ , where an increase in the carbon concentration lead to a

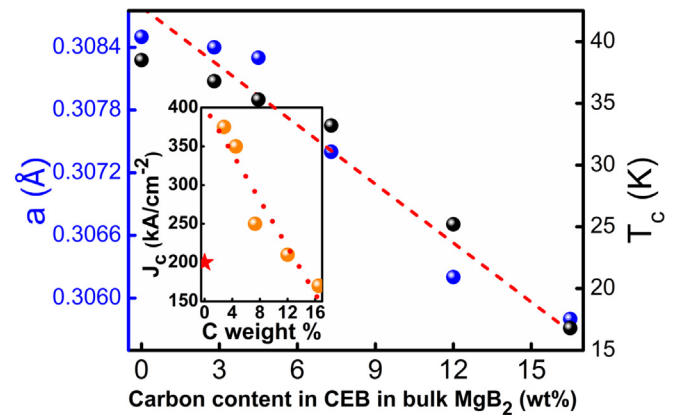


Fig. 1.  $a$ -axis lattice constant (solid blue spheres) and  $T_c$  (solid black spheres) versus the carbon content in CEB. Inset: Self-field  $J_c$  at 20 K versus CEB carbon content in the  $\text{MgB}_2$  samples. The red dashed lines are the guide to the eye and the solid star indicates the self-field  $J_c$  of the reference  $\text{MgB}_2$  sample at 20 K. (For interpretation of the references to colour in this figure legend, the reader is referred to the web version of this article.)

decrease in the  $a$ -axis lattice parameter and also to the suppression of  $T_c$  [20,34]. From the magnetization measurements, it is found that in the low doping levels of 2.8, 4.5, and 7.3 wt% C,  $T_c$  decreases moderately. However, for the samples with high carbon contents of 12 and 16.5 wt%,  $T_c$  decreases drastically as shown in Fig. 1.  $T_c$  dropped to 16 K for the sample with the highest carbon content of 16.5 wt% in CEB. A systematic decrease in  $T_c$  of the samples is an indication of the homogeneous substitution of boron by carbon in  $\text{MgB}_2$  [34]. Rapid decrease in  $T_c$  for the high doping levels of 12 and 16.5 wt%, can also be an indication of enhanced phase segregation.

Inset in Fig. 1 shows the self-field  $J_c$  at 20 K versus the carbon content in the initial CEB precursor. Obviously, the undoped reference sample (represented by a solid star in the inset of Fig. 1) has a low  $J_c$  value of 250  $\text{kA/cm}^2$  in self-field and at 20 K as compared to the doped samples. The sample with carbon content of 2.8 wt% in CEB exhibits a self-field  $J_c$  of 375  $\text{kA/cm}^2$  at 20 K. With increasing carbon content, however,  $J_c$  drops continuously. The sample with 16.5 wt% C showed a low self-field  $J_c = 180 \text{ kA/cm}^2$  and low  $T_c = 16 \text{ K}$ , reflecting degradation of the superconducting phase as a result of heavy carbon doping. Improvement of  $J_c$  and the degradation of  $T_c$  in these samples are notable, and therefore, further investigation of the evolution of grain size and the evolution of the  $E_{2g}$  Raman mode using AFM and the Raman spectroscopy were conducted.

### 3.2. AFM analysis

Fig. 2 shows the results of AFM topographic observation for (a)  $\text{MgB}_2$  reference sample (b) 2.8 wt%, (c) 4.5 wt%, (d) 7.3 wt%, (e) 12 wt% and (f) 16.5 wt% carbon content in CEB. The histograms represent the grain size distribution. Histogram labelled (a) and (b) represents the grain size distribution in the reference  $\text{MgB}_2$  and the sample with 2.8 wt% carbon in CEB sample, respectively, whereas the histogram (c) represents the grain size distribution for the AFM image (c). The grain size distributions for other samples (7.3, 12, and 16.5 wt%) were similar to that of the 4.5 wt% sample. Prior to the AFM studies, the samples with dimensions of  $1.5 \times 1.5 \times 1 \text{ mm}^3$  were cut from the pellet and polished. Since the fabricated samples were highly porous, a very careful sample polishing was necessary. Each sample was subjected to several rounds of dry polishing using lapping films of various mesh sizes (12, 5, 3, 1 and 0.3  $\mu\text{m}$ ). The surfaces of the final samples were mirror polished. Grain size

Download English Version:

<https://daneshyari.com/en/article/5458764>

Download Persian Version:

<https://daneshyari.com/article/5458764>

[Daneshyari.com](https://daneshyari.com)